Final Report to AFOSR/AOARD

Development of Ultra-fine Grained Ti and Ti-6Al-4V alloy by Equal Channel Angular Extrusion

For the period

1 November 2001 to 31 October 2002
(12 months)

DISTRIBUTION STATEMENT A
Approved for Public Release
Distribution Unlimited

submitted by

Professor Dong H. Shin
Department of Metallurgy and Materials Science
Hanyang University, Ansan 425-791, Korea

21 February 2003

20041119 034

REPORT DOCUMENTATION PAGE

Form Approved

OMB No. 0704-0188

The public reporting burden for this collection of information is estimated to average 1 hour per response, including the time for reviewing instructions, searching existing data sources, gathering and maintaining the data needed, and completing and reviewing the collection of information. Send comments regarding this burden estimate or any other aspect of this collection of information, including suggestions for reducing the burden, to Department of Defense, Washington Headquarters Services, Directorate for Information Operations and Reports (0704-0188), 1215 Jefferson Davis Highway, Suite 1204, Arlington, VA 22202-4302. Respondents should be aware that notwithstanding any other provision of law, no person shall be subject to any penalty for failing to comply with a collection of information if it does not display a currently valid OMB control number.

PLEASE DO NOT RETURN YOUR FORM TO THE ABOVE ADDRESS.

1. REPORT DATE *(DD-MM-YYYY)*	2. REPORT TYPE	3. DATES COVERED *(From - To)*
12-03-2003	Final	01-Nov-01 to 31-Oct-02

4. TITLE AND SUBTITLE

Development of Ultrafine-Grained Ti and Ti-6Al-4V Alloy by Equal Channel Angular Extrusion

5a. CONTRACT NUMBER

F6256202P0230

5b. GRANT NUMBER

5c. PROGRAM ELEMENT NUMBER

6. AUTHOR(S)

Prof. Dong H. Shin

5d. PROJECT NUMBER

5e. TASK NUMBER

5f. WORK UNIT NUMBER

7. PERFORMING ORGANIZATION NAME(S) AND ADDRESS(ES)

Hanyang University
Kyunggi-Do
Ansan 425-791
Korea (South)

8. PERFORMING ORGANIZATION REPORT NUMBER

N/A

9. SPONSORING/MONITORING AGENCY NAME(S) AND ADDRESS(ES)

AOARD
UNIT 45002
APO AP 96337-5002

10. SPONSOR/MONITOR'S ACRONYM(S)

AOARD

11. SPONSOR/MONITOR'S REPORT NUMBER(S)

AOARD-014027

12. DISTRIBUTION/AVAILABILITY STATEMENT

Approved for public release; distribution is unlimited.

13. SUPPLEMENTARY NOTES

14. ABSTRACT

This report covers efforts to use equal-channel angular extrusion (ECAE) to produce a fine-grained structure in Ti and Ti-6Al-4V. Both materials were successfully produced. Details of processing and resulting microstructures (phase morphology, grain size, texture, dislocation and twin substructures) are presented and discussed. Ti alloys are a mixture of hexagonal-close-packed and body-centered-cubic crystal structures. Plastic deformation is accommodated by a mixture of dislocation motion and twinning.

15. SUBJECT TERMS

Titanium Alloy, Materials Processing, Structural Materials

16. SECURITY CLASSIFICATION OF:			17. LIMITATION OF ABSTRACT	18. NUMBER OF PAGES	19a. NAME OF RESPONSIBLE PERSON
a. REPORT	b. ABSTRACT	c. THIS PAGE			Kenneth C. Goretta, Ph.D.
U	U	U	UU	26	19b. TELEPHONE NUMBER *(Include area code)* +81-3-5410-4409

Contents

Final Report on

Development of Ultra-fine Grained Ti and Ti-6Al-4V alloy by Equal Channel Angular Extrusion

Chapter 1: Introduction

It has been demonstrated by various researchers that equal channel angular extrusion (ECAE) of structural materials leads to refinement of grains to a range from tens to hundreds of nanometer. The grain refinement has been regarded as the most viable method for development of the advanced structural materials having a combination of properties i.e., high specific strength and good plastic deformability.

The primary objective of this research was to provide a fundamental understanding on the processing science necessary to produce ultra-fine grained (UFG) commercially-pure (CP) Ti and Ti-6Al-4V alloy using equal channel angular extrusion (ECAE) process. Major achievements of this research are summarized as follows:

1) Strain accommodation mechanism during ECAE of titanium was investigated.

Our ECAE studies on CP titanium showed that titanium deforms via entirely different mechanisms compared with those of FCC or BCC metals such as aluminum, copper and steel. During the first ECAE pass, the strain imposed by ECAE was accommodated mainly by {1011} deformation twinning. After the first ECAE pass, however, strain was accommodated primarily by dislocation slip on a system which dependant on processing routes of ECAE. In addition, texture developed during the first pass plays an important role in determining the slip systems. This new finding should shed some light on grain refining mechanisms of Ti during ECAE.

2) Microstructure development of Ti-6Al-4V alloy during ECAE was investigated.

Effects of pressing temperature and initial microstructure on ECAE of Ti-6Al-4V alloy were also investigated. The ECAE was carried out isothermally using samples with two typical microstructures, i.e., Widmanstätten microstructure and equiaxed microstructure. The results indicated that the initial microstructure plays an important role in the development of microstructure during the first pass, but its effect diminished with increase in ECAE passes. Collaborative research with Dr. Semiatin showed that the effects could be attributed to flow softening phenomenon.

Chapter 2: Microstructure development during equal channel angular pressing of titanium

Available online at www.sciencedirect.com
SCIENCE DIRECT®
Pergamon
Acta Materialia 51 (2003) 983–996
Acta MATERIALIA
www.actamat-journals.com

Microstructure development during equal-channel angular pressing of titanium

D.H. Shin [a,*], I. Kim [a], J. Kim [a], Y.S. Kim [b], S.L. Semiatin [c]

[a] *Department of Metallurgy and Materials Science, Hanyang University, Ansan, Kyunggi-Do 425-791, South Korea*
[b] *Department of Materials Science and Engineering, Hongik University, Seoul 121-791, South Korea*
[c] *Air Force Research Laboratory, Materials and Manufacturing Directorate, AFRL/MLLM, Wright-Patterson Air Force Base, OH 45433, USA*

Received 27 July 2002; received in revised form 22 October 2002; accepted 24 October 2002

Abstract

The development of microstructure during equal-channel angular pressing (ECAP) of commercial-purity titanium was investigated to establish the mechanisms of grain refinement and strain accommodation. Samples were deformed at 623 K via three different processing routes: A, B, and C. After the first pass, transmission electron microscopy (TEM) revealed that the strain imposed by pressing was accommodated mainly by $\{10\bar{1}1\}$ deformation twinning. During the second pass, the deformation mechanism changed to dislocation slip on a system which depended on the specific route. For route C, prism (**a**) and pyramidal (**c** + **a**) slip occurred within alternating twin bands. For route B, prism **a** slip was the main deformation mechanism. For route A, deformation was controlled by basal **a** slip and micro-twinning in alternating twin bands. The variation in deformation behavior was interpreted in terms of the texture formed during the first pass and the Schmid factors for slip during subsequent deformation.
© 2002 Acta Materialia Inc. Published by Elsevier Science Ltd. All rights reserved.

Keywords: Equal-channel angular pressing; Titanium; Twinning; Slip; TEM

1. Introduction

Equal-channel angular pressing (ECAP) has attracted much attention because of its usefulness in producing bulk materials with ultra-fine-grain (UFG) sizes in the range of 100–500 nm [1–5]. There have been many reports of UFG materials produced by the ECAP process; these materials include face-centered cubic (fcc) (e.g., Al alloys, Cu, Ni), body-centered cubic (bcc) (e.g., low-carbon steel) and hexagonal close packed (hcp) (e.g., magnesium alloys) metals [2–16]. During ECAP, a sample is passed through a die with two intersecting channels equal in cross section [4–8] and deformed via simple shear at the intersection of the channels [17–19]. Because the shearing process does not alter the dimensions of the sample, a large amount of plastic strain (true effective strains as large as 10–20) can be imposed via multi-pass processing. In addition, different microstructures and textures can be developed by changing the direc-

* Corresponding author. Tel.: +82-314 005 224; fax: +82-314 173 701.
E-mail address: dhshin@hanyang.ac.kr (D.H. Shin).

1359-6454/03/$30.00 © 2002 Acta Materialia Inc. Published by Elsevier Science Ltd. All rights reserved.
doi:10.1016/S1359-6454(02)00501-3

tion of shear via sample rotations about the longitudinal axis between passes [9,17,18].

The possible application of ECAP to hcp metals, such as titanium and its alloys, is challenging because the deformability of these materials is normally inferior to that of cubic metals. This behavior is mainly due to the fact that slip occurs primarily only on basal or prism planes along the close-packed (**a**) direction. In Ref. [20], for example, a slip in titanium was observed to occur along the $\langle 11\bar{2}0\rangle$ direction primarily on $\{10\bar{1}0\}$ planes and less frequently on the $\{0001\}$ plane. Since a slip does not induce a plastic strain along the **c** axis of the crystal, deformation twinning or **c** + **a** slip on pyramidal planes has been observed to accommodate the plastic strain imposed by conventional deformation processes [21–23]. The twinning planes in titanium are $\{10\bar{1}2\}$, $\{11\bar{2}1\}$, and $\{11\bar{2}2\}$ at ambient temperatures and $\{10\bar{1}1\}$ at temperatures above 673 K [24]. Furthermore, deformation twins have been found to enhance slip along the $\langle 11\bar{2}3\rangle$ direction (i.e., **c** + **a** slip) on $\{\bar{1}011\}$ or $\{\bar{1}\bar{1}22\}$ planes [23,24]. Several investigations have been conducted to find an effective ECAP route to refine the grain size and enhance the mechanical properties of titanium [11,25,26]. Among the various approaches, route B_c, in which the sample is rotated 90° clockwise between each pass, was found to be the most effective in refining the grain size [11]. The deformation temperature was found to affect grain refinement significantly as well [26].

Grain refinement during the ECAP of metals with cubic crystal structures is controlled by the formation of sub-boundaries with high dislocation densities [4,5]. By contrast, the deformation of titanium during ECAP may be expected to be quite different because it involves not only the slip of dislocations but also deformation twinning. Hence, the present work was undertaken to establish the deformation mechanisms of titanium during ECAP in order to provide insight into optimal methods for grain refinement and the improvement of mechanical properties. For this purpose, commercially pure titanium was pressed 1 or 2 passes via three different ECAP routes (A, B, and C). The microstructure changes during the early stage of ECAP are usually very great and often influence microstructure evolution during subsequent passes. Microstructure development was determined using optical, scanning electron, and transmission electron microscopy as well as X-ray diffraction (XRD).

2. Materials and procedures

The program material consisted of bar stock of commercial-purity titanium (grade 2) with an average grain size of 30 μm. Its composition (in weight percent) was 0.07 iron, 0.009 nitrogen, 0.012 hydrogen, 0.10 oxygen, balance titanium. Cylindrical samples measuring 18 mm diameter×130 mm length were machined from a titanium bar. Before ECAP, the samples were annealed at 1073 K for 1 h under an argon atmosphere in order to remove any residual hot work. After annealing, the texture of the material was weak.

A detailed description of the ECAP apparatus used in this study can be found elsewhere [4]. In brief, the ECAP die was designed to yield a shear strain of ~1.83 during each pass [27]. It contained an inner contact angle (Φ) and arc of curvature at the outer point of contact between the channels (Ψ) of 90 and 20°, respectively. Pressing through a single pass or two passes was conducted at 623 K at a constant pressing speed of 2 mm/s. The pressing temperature was chosen to avoid shear localization that characterizes ECAP of commercial-purity titanium at temperatures between 298 and 598 K [28]. Macroscopic shear patterns produced by pressing routes A, B, and C are illustrated schematically in Fig. 1a, b. The deformation characteristics of routes A, B, and C have been described previously in the literature [27,29,30].

Following ECAP, microstructural observations were made using specimens cut either parallel or normal to the longitudinal axis as shown in Fig. 1; here X is the plane perpendicular to the longitudinal axis of the sample, and Y and Z are the planes parallel to the size faces and to the top face at the point of exit from the die, respectively. For optical and scanning electron microscopy (SEM) examination, samples were polished and etched with a solution of 4% HF, 20% perchloric acid, and 76% distilled water. Specimens for transmission elec-

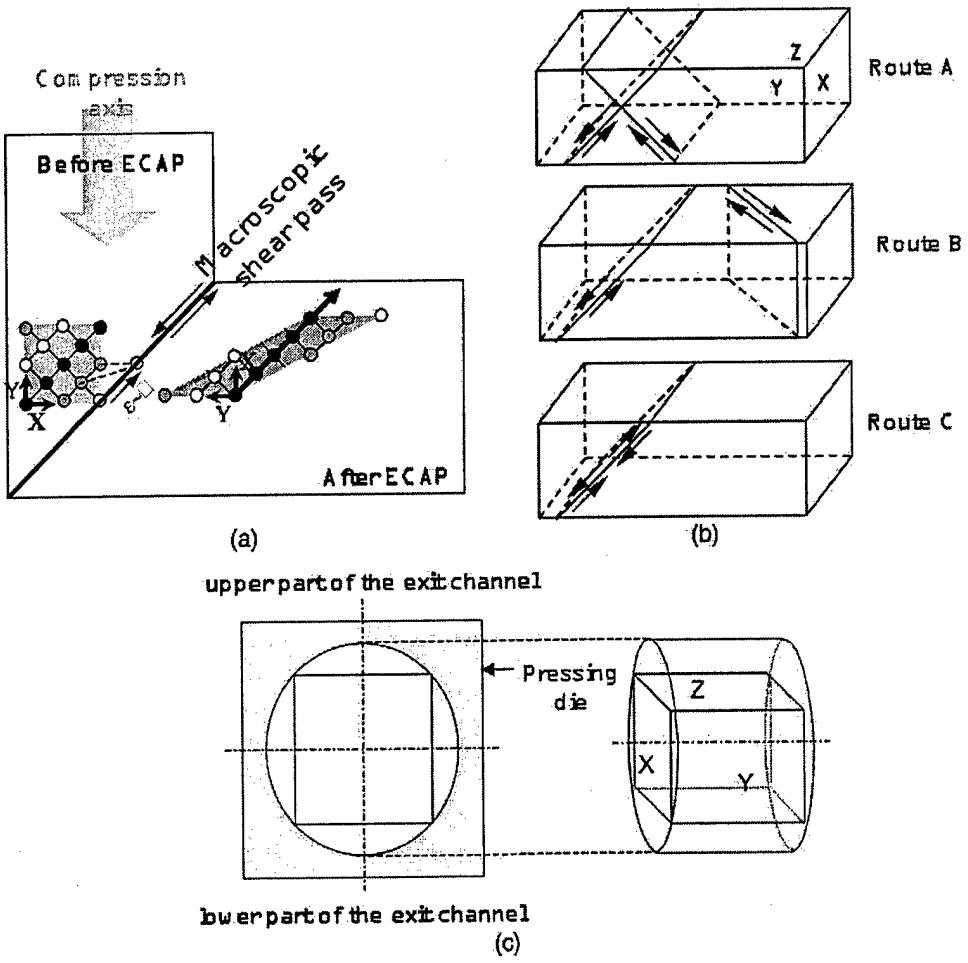

Fig. 1. (a) Macroscopic shearing path associated with a single passage. (b) Macroscopic shearing patterns associated with different processing routes. (c) Schematic diagram of the sectioning of pressed samples for microstructural observation.

tron microscopy (TEM) were prepared by mechanically thinning samples to ~40 μm followed by twin jet polishing with a solution of 5% perchloric acid, 35% butanol, and 60% methanol. Polishing was conducted at 233K using a voltage of 40V. TEM images and corresponding selected area diffraction (SAD) patterns of each sample were obtained at 200 kV in a JEOL JEM 2010. XRD analyses were conducted to determine the texture of the samples prior to and after pressing.

3. Results

3.1. Microstructure developed during the first ECAP pass

Fig. 2a shows an optical micrograph of the as-annealed titanium used as the starting material. The grain structure was equiaxed with an average size of ~100 Pm. During the first ECAP pass, fine microstructural features inclined ~30° to the longitudinal direction were developed (Fig. 2b). (The micrograph in Fig. 2b was taken from the *Y* plane.

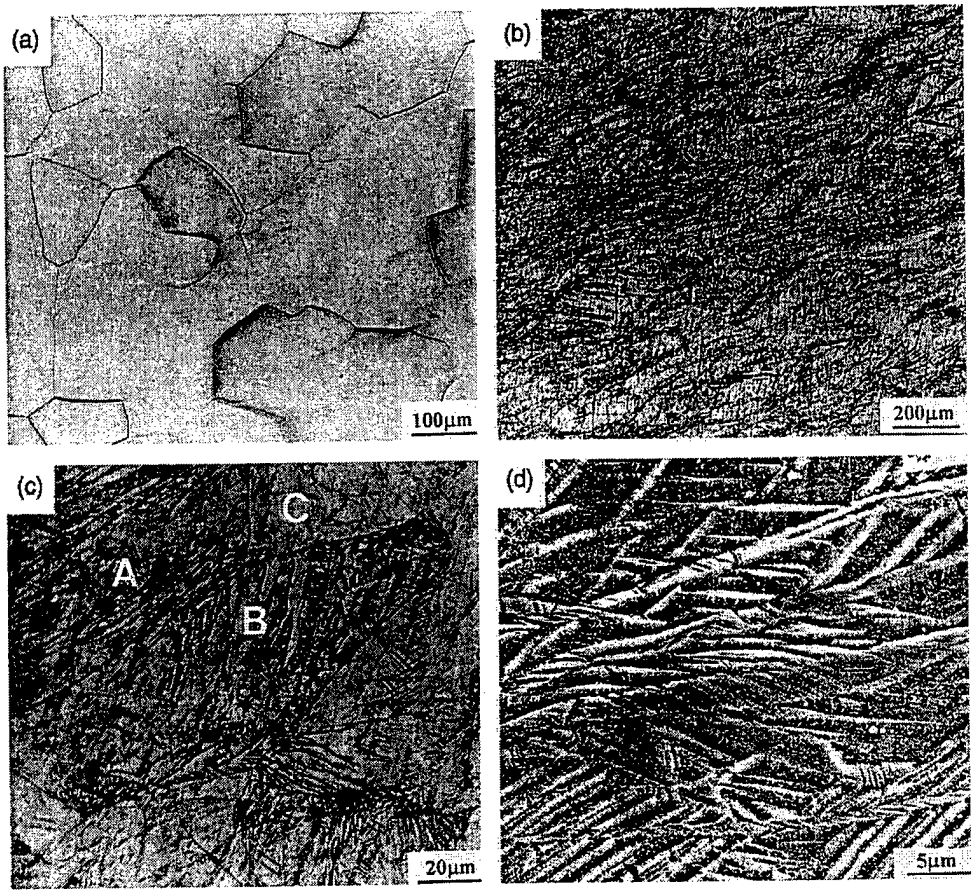

Fig. 2. Optical and SEM micrographs of as-annealed and as-pressed (single pass) Ti: (a) as-annealed and (b–d) as-pressed.

Hereafter, the plane of micrograph is the Y plane unless specified otherwise.) A homogeneous shear strain of 1.83 would produce a microstructural texture lying at 28.6° ($= 90 - \tan^{-1} 1.83$) to the longitudinal direction. Hence, the directionality of this macrostructure is reasonable. The morphology of the inclined features was similar to the flow lines observed in metals with fcc and bcc crystal structures after a single ECAP pass [7,8,26,29]. Initially, the flow lines were attributed to the formation of fine shear bands during the pressing operation. Observation of the fine features in titanium at a higher magnification, however, revealed that they consisted of deformation twins (Fig. 2c). In particular, grains with three distinct microstructures, marked A, B, and C, were observed. In A, twins spanning the entire grain were formed parallel to the flow lines. On the other hand, the twins in B were inclined approximately 40° to the orientation of the deformation zone of the pressing, and were observed to include micro-twins inside. Inasmuch as the optical microstructure of C was not as evident as those of A and B, SEM observation of this region was required for a detailed analysis (Fig. 2d). As shown in the figure, the grain contained micro-twins whose width was less than 1 μm. Thus, all of the observations after the first ECAP pass revealed deformation twins either on a macro- or a micro-scale.

A TEM micrograph of the structure developed during the first ECAP pass is shown in Fig. 3. Elongated parallel bands with a width of ~0.07 Pm were observed. These bands were similar in appearance to slip bands formed in cubic metals [4,5,17], but were much finer. The width of the slip bands in the previous work was generally greater

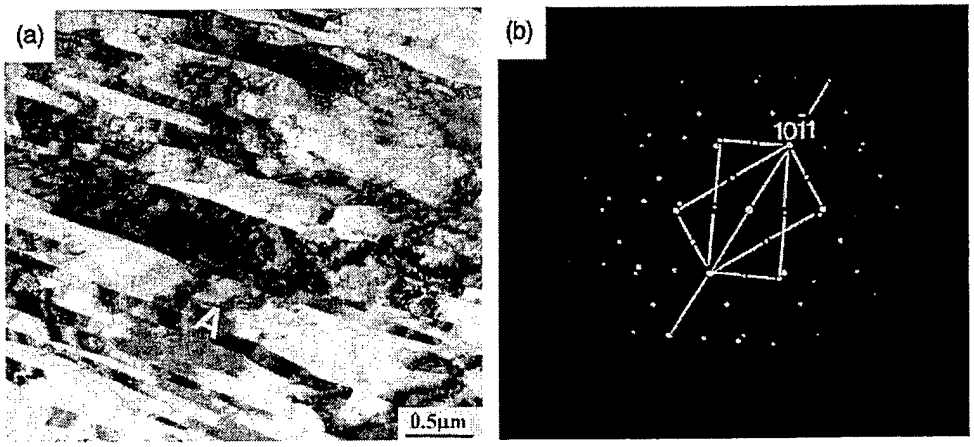

Fig. 3. (a) TEM micrograph of Ti after a single ECAP pass and (b) the corresponding SAD pattern.

than 0.2 Pm. A SAD pattern from a region containing two adjacent bands (marked "A" in Fig. 3a) was taken using a [$\bar{1}2\bar{1}0$] zone axis (Fig. 3b). The mirror spots of the [$\bar{1}2\bar{1}0$] diffraction pattern appeared with respect to the (10$\bar{1}$1) plane, indicating that the two adjacent bands constituted a {10$\bar{1}$1} twin structure. The same twin system was consistently observed for more than 50 different regions, even from twins aligned differently in the same grain. In addition, the dislocation density within the bands was approximately $10^{13}/m^2$, a value much lower than that typically developed in heavily deformed cubic metals, i.e., ~$10^{15}/m^2$ [1,4]. No indication of a reduction in dislocation density via recovery was found in the TEM micrographs.

These results suggest that titanium deforms *primarily* via {10$\bar{1}$1} deformation twinning during the first ECAP pass, rather than by slip as is found in cubic materials [7,8,26,29]. This result differs with previous findings that titanium deforms mainly by slip of a-type dislocations above ambient temperature and that twinning assists the activation of secondary slip systems [20,21]. Furthermore, deformation twins were found only on {10$\bar{1}$1} planes, even though samples were pressed at 623 K. A previous report indicated that deformation twinning on {10$\bar{1}$1} planes was preferred at temperatures *above* 673 K [21]. Twins on {10$\bar{1}$2}, {11$\bar{2}$1}, and {11$\bar{2}$2} planes have been reported to occur at lower temperatures. Several factors, including the constraint imposed during the pressing, the shear mode of deformation, and the large shear and high shear rate, may have induced the {10$\bar{1}$1} twinning system to operate at lower temperature. In addition, the shear strain that is developed by {10$\bar{1}$1} deformation twinning has been reported to be only ~0.1 [31], or a level which is much smaller than that imposed by the ECAP, ~1.83. The mode of deformation twinning during ECAP, therefore, must be different from that observed in conventional deformation processes. Thus, further detailed study of the source of this behavior is warranted.

In order to investigate texture formation during ECAP, texture analyses were conducted on samples in the as-annealed condition as well as after the first ECAP pass (Fig. 4). In Fig. 4a, the (10$\bar{1}$0) pole figure, taken from a plane normal to the extrusion direction, shows that the texture of the annealed sample is weak. This indicates that the annealing treatment removed any remnants of a possible fiber texture in the as-received material. After the first ECAP pass, however, a strong (0002) texture was observed (Fig. 4b). The texture formed during the first ECAP pass may also have played an important role in the transition in the deformation mode.

3.2. Microstructures developed during the second ECAP pass

The microstructure developed during the second ECAP pass was a strong function of the specific processing route. The structures that were

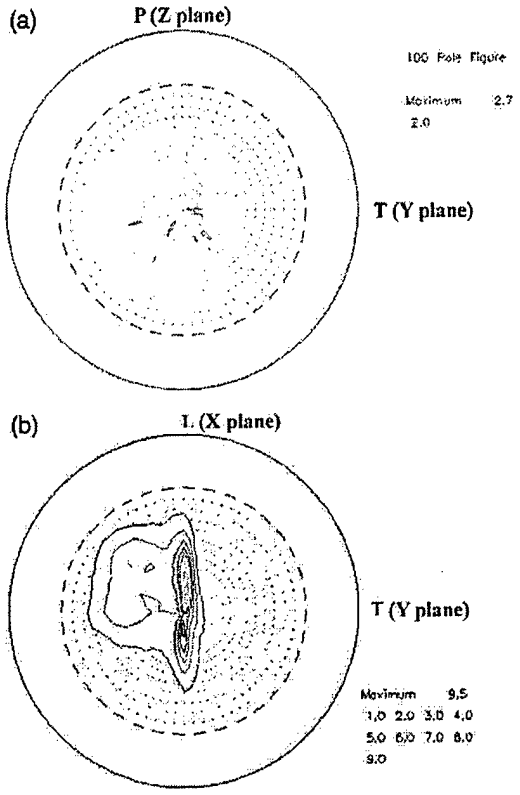

Fig. 4. Pole figures of Ti: (a) from a cross section of extruded bar after annealing, (b) from a longitudinal section after a single pass.

developed are summarized in the sections that follow.

3.2.1. Route C

Optical and SEM micrographs of the structure developed during the second pass via route C (in which the shear is fully reversed during successive passes by 180° rotation of the billet between passes, Fig. 1a) are shown in Fig. 5a, b. After the second pass, the flow lines associated with the simple shear deformation of the first pass appeared to be randomly oriented, thus resulting in a relatively homogeneous microstructure (Fig. 5a). This observation is in accord with the fact that the original macrostructure tends to be restored after every *even* pass of route C [3–7]. Nevertheless, an SEM micrograph at higher magnification (Fig. 5b) revealed remnants of micro-twins, which were severely distorted and segmented compared with those after the first pass (Fig. 2d).

Fig. 5c shows a TEM micrograph and SAD pattern of the sample given two passes via route C. As shown in the figure, the dislocation density was increased significantly compared to that in Fig. 3a. The SAD pattern taken parallel to the $[\bar{1}2\bar{1}0]$ zone axis from the region marked "A" in Fig. 5c revealed that the band still had the $\{10\bar{1}1\}$ twin plane, although the plane was slightly misaligned by ~3°. Hence, dislocation activity during the second pass must have rotated the twins developed during the first pass.

In order to analyze the characteristics of the dislocations in the twin bands, two-beam TEM images were taken with the $(10\bar{1}0)$ (Fig. 5d, e) and (0002) (Fig. 5f) beam, respectively. The two-beam images with $(10\bar{1}0)$ and (0002) spots can reveal dislocations of **a** slip and **c** + **a** slip character, respectively [21]. From Fig. 5e, f, it was determined that twin bands with numerous **a** dislocations alternated with bands with numerous **c** + **a** dislocations.

In the twin bands, low angle boundaries were surrounded with dislocations of **a**-slip character, as shown in Fig. 5d, e. In addition, the low-angle boundaries in Fig. 5d (indicated by arrows) were aligned approximately normal to the **g** vector of $\langle 10\bar{1}0\rangle$ and were found to be parallel to the [0002] direction [29,30]. This indicates that a slip occurred on $\{10\bar{1}0\}$ planes, or the main slip system commonly found for titanium. In addition, the micrographs showed that the dislocations were blocked at the twin boundaries. This indicates that twin boundaries acted as obstacles for dislocation movement. This phenomenon has been generally observed in hcp metals plastically deformed by rolling or drawing [32,33]. Fig. 5f shows an enlarged dark field image of a twin band containing **c** + **a** dislocations. In this band, the density of **c** + **a** dislocations was very high, and most of them were aligned parallel to the twin boundary without the formation of low-angle boundaries.

3.2.2. Route B

Optical and SEM micrographs of the structure developed during the second pass via route B (in which the billet is rotated 90° after the first pass) are shown in Fig. 6a, b. Alignment of the metal

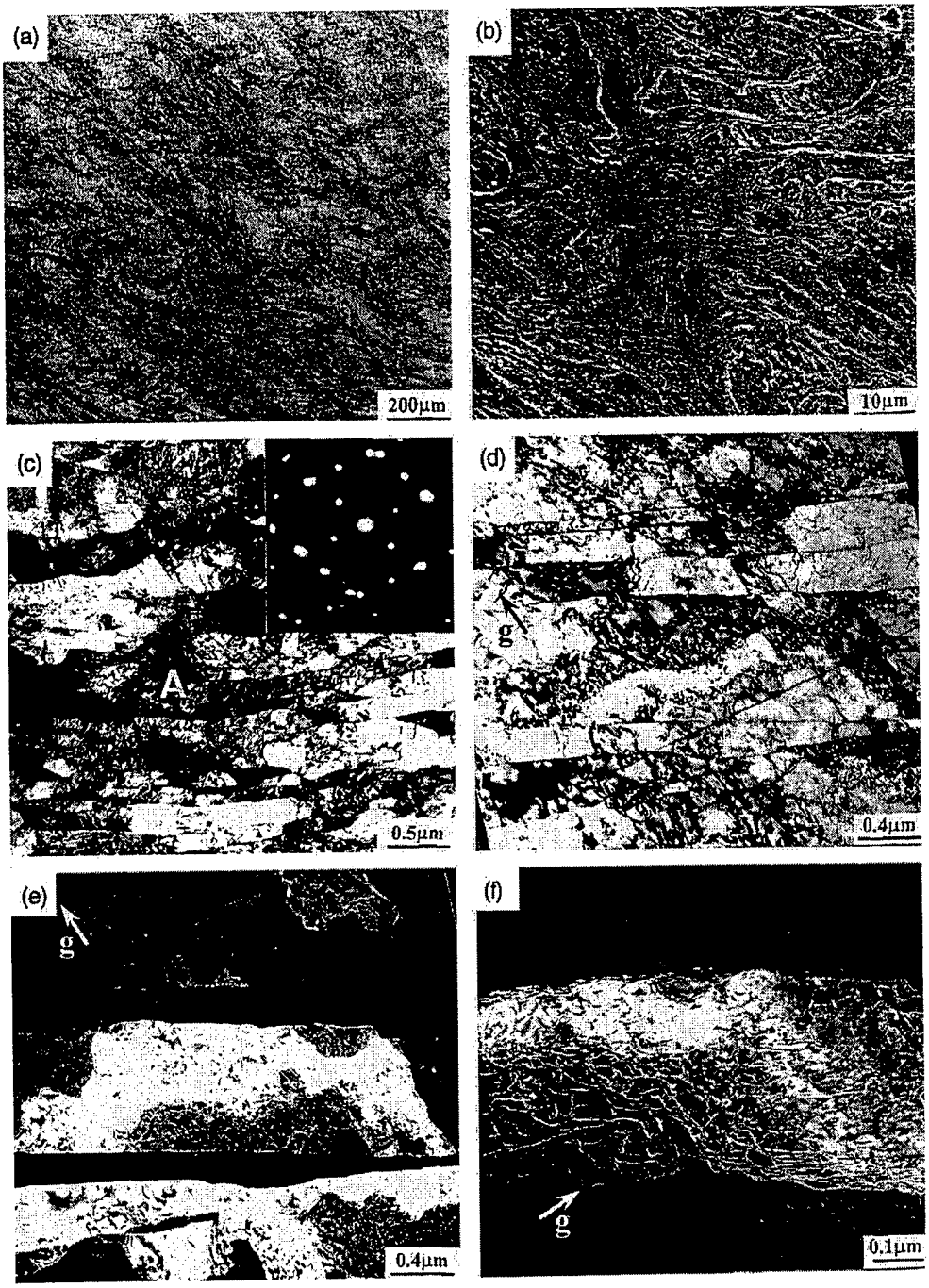

Fig. 5. Micrographs of Ti after the second ECAP pass via route C: (a) optical, (b) SEM, and (c) TEM with SAD pattern; and (d) $(10\bar{1}0)$ bright field, (e) $(10\bar{1}0)$ dark field, and (f) (0002) dark field images.

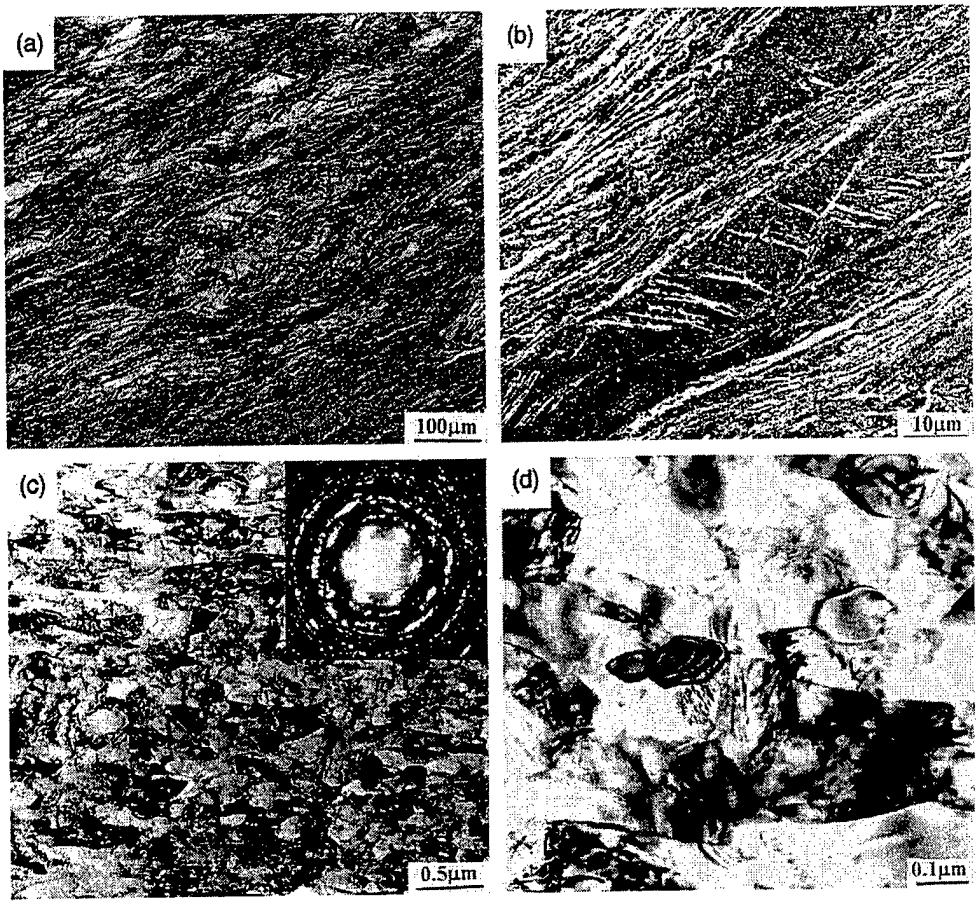

Fig. 6. Micrographs of Ti after the second ECAP via route B: (a) optical, (b) SEM, (c) TEM with SAD pattern, and (d) TEM (higher magnification).

flow lines after the second pass remained almost the same as after the first pass except the spacing was decreased. SEM observation of the sample revealed that most of the shear traces were aligned parallel to the orientation of the deformation zone of the second pass. Fig. 6c, d shows TEM micrographs and the corresponding SAD pattern of the sample after the second pass via route B. Nearly equiaxed grains approximately 0.07 μm in diameter were formed; some of these grains had a high dislocation density. When examined under two-beam dark field imaging conditions, most of the dislocations were found to be **a**-type.

The SAD pattern of the sample in Fig. 6c consisted of a number of strong spots diffused at an angle of ~15°. This angle is the maximum angular difference between grains within the viewing area of the SAD and indicates that most of the neighboring grains have characteristics of low-angle boundaries. Although characteristic mirror-type diffraction spots from a twinning system were not evident, strong $\{10\bar{1}1\}$ spots to its normal direction were formed, indicating that the bands were formed on $\{10\bar{1}1\}$ planes. In addition, the thickness fringes in the vicinity of the band boundaries were narrow, probably due to a parallel alignment of the band interfaces to the beam direction. These results indicate that the bands may have been the remnant of deformation twin bands from the first ECAP pass. The twin bands would have been rotated and distorted severely during the second pass. A TEM micrograph at a higher magnification (Fig. 6d) showed fine grains near coarse ones with well-developed grain boundary fringes. Convergent

beam electron diffraction (CBED) analysis confirmed that most of the fine grains had boundaries which were high-angle in character.

3.2.3. Route A

Optical and SEM micrographs of the structure developed during the second pass via route A (in which the billet is not rotated between passes) are shown in Fig. 7a, b. As expected, the metal flow lines were inclined at a greater angle to the longitudinal axis of the sample, and their spacing became more homogenous. A homogeneous shear strain of 3.66 ($= 2 \times 1.83$) would produce an inclination of $90° - \tan^{-1} 3.66 = 15.3°$, in approximate agreement with the observed macrostructure. The SEM micrograph revealed that most of the shear traces consisted of micro-twins nearly aligned to the longitudinal direction. Some of the twins, however, were aligned approximately 45° to the direction of the shear traces, which is similar to grain B of the sample after the first pass (Fig. 2b). The alignment of the shear traces after the second pass was more pronounced and their pitch was finer compared with that after the first pass. The increased alignment of shear bands to the longitudinal direction in aluminum alloys and carbon steels processed via route A has also been observed [9,30].

Fig. 7c shows TEM micrographs and the corresponding SAD pattern of the sample processed by route A. The width of the twin bands was reduced to approximately 0.05 μm after the second pass. The SAD pattern of the sample showed that the twin plane was unchanged from the first pressing,

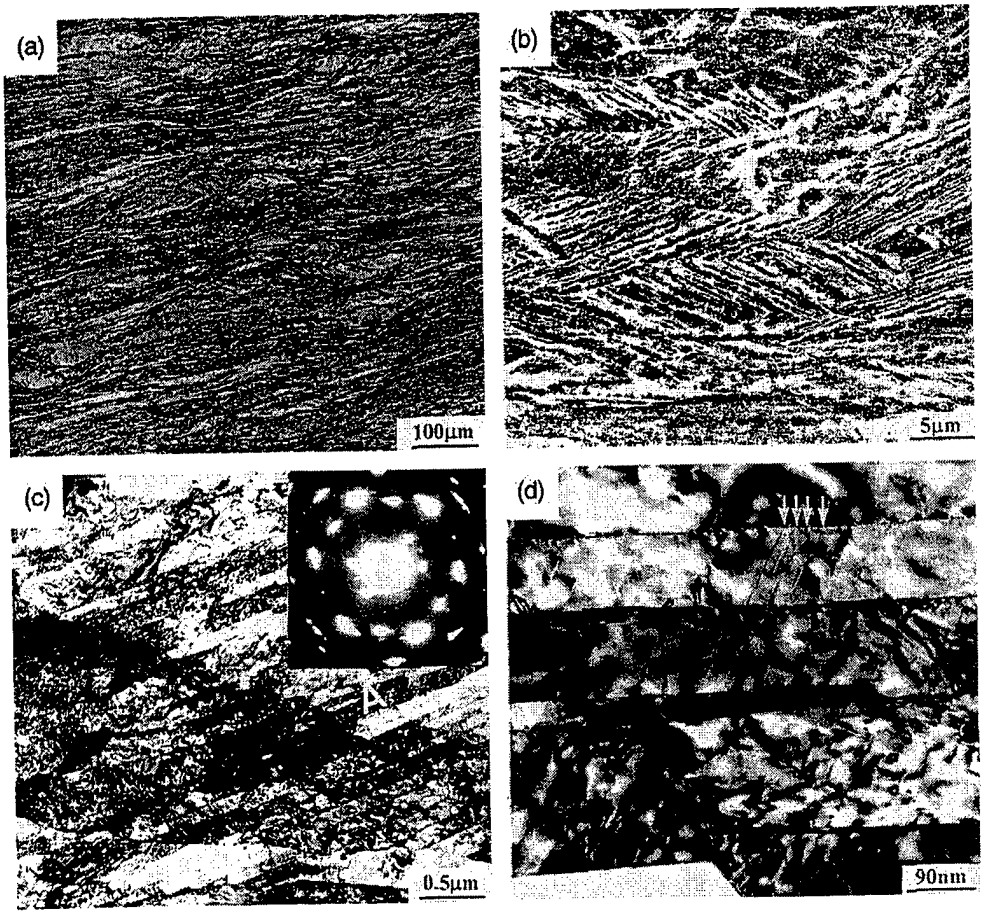

Fig. 7. Micrographs of Ti after the second ECAP pass via route A: (a) optical, (b) SEM, (c) TEM with SAD pattern, and (d) TEM (higher magnification).

i.e., $\{10\bar{1}1\}$. The spots of the SAD pattern, however, were diffused by an angle of ~ 5°, indicating that the twin bands were rotated slightly during the second pass. The dislocations in the bands were distributed uniformly and were determined to be a slip in character from two-beam dark field images. As shown in Fig. 7d, $\{10\bar{1}1\}$ micro-twins (indicated by arrows in the figure), aligned ~60° to the band direction, were clearly observed within the twin bands. Such micro-twins were not observed in samples processed via routes B or C.

4. Discussion

4.1. Deformation mechanism during the first ECAP pass

During the deformation of hcp metals, dislocation glide typically accommodates most of the imposed strain, and deformation twinning assists in the activation of secondary slip systems at temperatures higher than ambient. During the ECAP of commercial-purity titanium, however, the shear strain imposed during the initial pass (~1.83) appeared to be accommodated mainly by twinning on $\{10\bar{1}1\}$-type planes. In the twin bands, the dislocation density was approximately $10^{13}/m^2$, which is significantly lower than that observed in steel after a single ECAP pass, namely, 10^{15}~$10^{16}/m^2$. The measured dislocation density in the present work seems to be too low to accommodate the shear strain imposed by the pressing, ~1.83. Therefore, titanium during the first ECAP pass must have deformed mainly by twinning, rather than by slip associated with the glide of dislocations. In previous work, the high strain rate deformation of titanium with a coarse grain structure has been reported to promote deformation twinning even at high temperatures [33]. In the present work, the strain rate during ECAP was estimated to be ~10^{-1} s^{-1} [34], which should not have promoted deformation twinning.

Paton and Backofen [21,31] concluded that the $\{10\bar{1}1\}$ twinning (the so-called "b4" mode) of high-purity, single crystalline alpha titanium can accommodate a shear strain of only ~0.1. Therefore, the shear strain associated with twinning via the b4 mode is not large enough to accommodate the strain imposed by a single ECAP pass. Even if several different twins of $\{10\bar{1}1\}$ family were to have been activated in each grain, the total strain that would have been accommodated would have been much less than that imposed. These observations, i.e., low dislocation and high twin density in the pressed sample, suggest that the imposed strain should have been accommodated by twinning, especially by the $\{10\bar{1}1\}$ type. Therefore, it seems that a different type of $\{10\bar{1}1\}$ twinning modes must have been involved in the severe plastic deformation of titanium during ECAP. A previous study showed that there are other possible $\{10\bar{1}1\}$ twinning modes, i.e., the so-called b3 or b1 modes, in which the shear strain is ~0.55 and ~1.44 [35]. These values are comparable with the shear strain imposed by the ECAP, i.e., ~1.83. As discussed in Refs. [30,36], these modes are not preferred ones due to the highly distorted state of core configuration, i.e., higher interfacial energy. The analysis, however, was conducted by assuming negligible disturbance of atomic arrangement and no other deformation mechanism except twinning. On the other hand, the present investigation revealed that the new twinning modes, i.e., b3 or b1, might operate with atomic rearrangement comprising severe distortion during ECAP.

4.2. Deformation mechanism during the second ECAP pass

As shown in Figs. 5–7, after the second ECAP pass, the density of dislocations with **a** or **c** + **a** slip directions had increased significantly and the density of twin bands remained almost the same compared with that developed during the first pass. This suggests that plastic strain is mainly accommodated by slip, rather than by deformation twinning, during the second pass. Hence, the microstructural changes that occurred during the first pass, such as grain-size refinement and texture formation, must have increased the critical resolved shear stress (CRSS) for twinning over that for dislocation slip. The grain size dependence of the CRSS for twinning has been described very well with the Hall–Petch relation. The slope of the relation for twinning has been determined to be an

order of magnitude *larger* than that for slip, although the reason for this difference is not fully understood [37–39]. This indicates that the rate of increase in the twinning stress should be much larger than that of dislocation slip as the grain size decreases. The most significant change in deformation parameters between the first and second pass of ECAP was the effective grain size of the sample due to a fact that twin boundaries have been reported to act as obstacles for slip [32,33] and dislocations during ECAP were shown to be blocked by the twin boundaries in the present work (Figs. 5–7). Therefore, the critical resolved shear stress (CRSS) for twinning must have been increased much more significantly compared with that of dislocation slip as the effective grain size of the titanium alloy was decreased from 100 to 0.07 μm by ECAP, promoting the deformation by slip during the second pass.

Using the measured texture (Fig. 4) formed during the first ECAP pass, the resolved shear stress on each slip system for the three different routes used for the second ECAP pass was determined. This comprised the calculation of a ratio similar to the classical Schmid factor to quantify the ratio of the shear stress on a specific slip system to the applied macroscopic shear stress during ECAP. These calculations made use of the crystallographic relationship between the plane/direction of the shear stress imposed by the ECAP and the specific slip system to calculate the resolved shear stress. The relationship between the macroscopic shear direction and the resolved shear stress on a slip system is schematically illustrated in Fig. 8.

In route C, the macroscopic shear directions of the first and second pass are parallel to each other, but opposite in sense. Considering the $\{10\bar{1}1\}$ twins formed during the first pass, the crystal orientation during the second pass of ECAP can be illustrated schematically as in Fig. 9a. From the pole figure in Fig. 4, the normal direction of the Z plane after the first pass was aligned with the $\langle 10\bar{1}4\rangle$ direction. In the twinned region, the Schmid factor for a slip on prism planes was estimated to be larger than that for a slip on the basal plane and for **c** + **a** slip (Table 1). Because prism **a** is the easiest slip mode (i.e., has the lowest CRSS) in titanium, **a** slip on prism planes should be the main

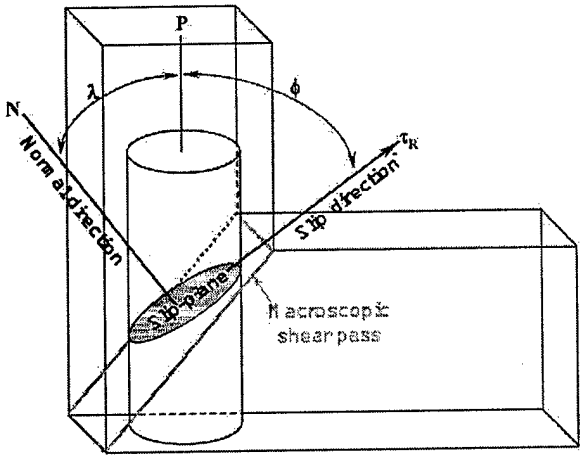

Fig. 8. Schematic diagram illustrating resolved shear stress on a slip system.

deformation mechanism in the twinned region. The increased mobility of dislocations of **a** type on prism planes should also favor the formation of subgrains in the twinned regions (Fig. 5d). On the other hand, in the matrix region, the Schmid factor for **c** + **a** slip was much larger than that of **a** slip because the basal and prism planes were close to normal and parallel to the pressing (longitudinal) direction, respectively. In addition, it has been reported that the CRSS for **c** + **a** slip above 600 K is similar to that for basal **a** slip [24]. Therefore, the matrix neighboring the twinned bands favored **c** + **a** slip. This crystallographic relationship should lead to the formation of alternating bands of either **a** or **c** + **a** dislocations, as was observed (Fig. 5).

In route B, the sample is rotated 90° about its longitudinal axis between passes, i.e., the Z plane is changed to the Y plane. A schematic diagram of such an atomic arrangement is illustrated in Fig. 9b. In this route, one of the $\{10\bar{1}0\}$ prism planes in the twinned region is inclined by ~30° to the longitudinal axis on the Y plane. Therefore, the Schmid factor for prism **a** slip is larger than that for any other deformation system, such as basal **a** slip, **c** + **a** slip, or $\{10\bar{1}1\}$ twinning. This is in good agreement with the dislocations observed using two-beam TEM images (Fig. 6). In the matrix, the $\{10\bar{1}0\}$ plane is inclined to the Y plane, but the resolved shear stress on this plane

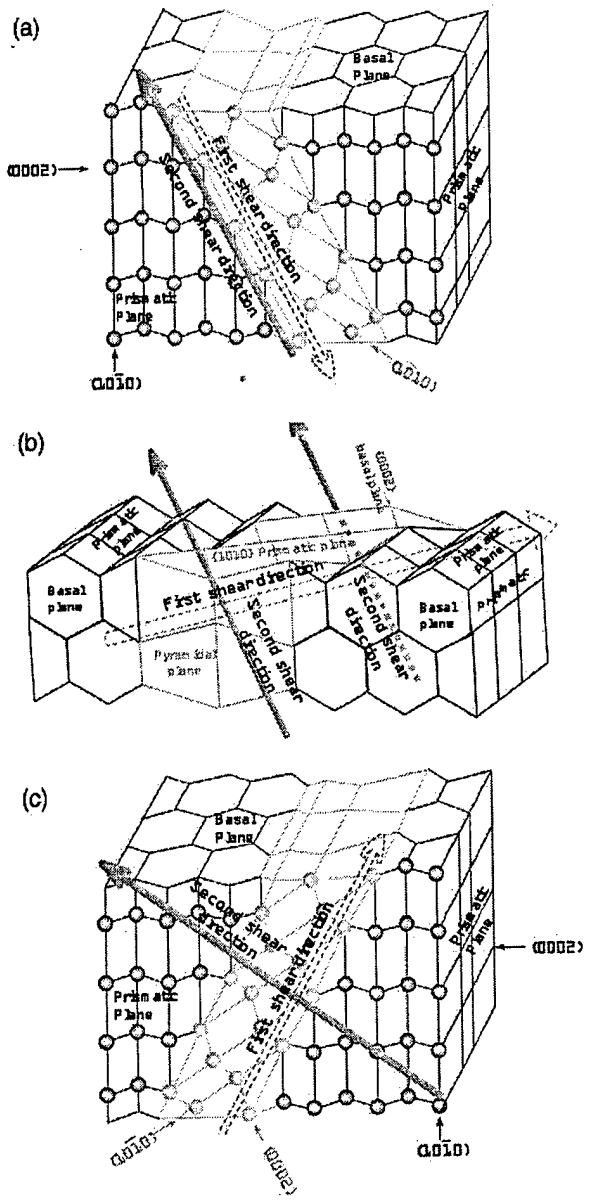

Fig. 9. Schematic diagrams illustrating the relationship between the crystal orientation and the macroscopic shear directions during the second ECAP pass: (a) route C, (b) route B and (c) route A. (—(black line), matrix region; —(grey line), twinned region).

remains the same as that for the most highly stressed prism plane in the twinned region. Therefore, prism **a** slip in the matrix would be feasible, but the slip plane in the matrix is not parallel to that in the twinned region. This type of slip mode was observed indirectly in region A of Fig. 6; the fringes of grain boundaries indicated that low angle boundaries in one twin band were parallel to the $(10\bar{1}0)$ beam direction, and those in the others were inclined. In addition, the crystallographic orientation between two adjacent twins makes it easy for dislocations to slip on the prism planes in each of the twins. This may promote the formation of small subgrains by dislocation cross slip (Fig. 6d).

In route A, the macroscopic shear direction of the second pass is parallel to that of the first pass. In this case, the prism plane is inclined 28.6° to the twin plane in the matrix region (Fig. 9c) and has a *smaller* Schmid factor than that associated with slip on the basal plane. The CRSS of basal slip has been reported to be similar to that for prism **a** slip at temperatures above 673 K [11,24]. Therefore, basal **a** slip may become the dominant slip mode in the matrix region. In addition, the cross slip of **a**-type dislocations on basal planes is very limited due to the *c*-axis anisotropy, a factor which may explain why the formation of subgrains was not observed (Fig. 7). The lack of cross slip should also promote dislocation pileups at twin boundaries and cause a strong stain field at the twin boundaries, which may act as a source for deformation in neighboring layers, i.e., produce new $\{10\bar{1}1\}$ micro-twins inside the original twins (Fig. 7d). In the twinned region, **c** + **a** slip on the $\{10\bar{1}1\}$ plane has a larger Schmid factor than prism or basal **a** slip, and thus **c** + **a** dislocations were observed here.

5. Summary

The slip and twinning behavior in commercial-purity titanium was determined to elucidate the mechanisms of microstructure development during the ECAP process. During the first ECAP pass, titanium was observed to deform by deformation twinning. TEM analysis revealed that twinning occurred on $\{10\bar{1}1\}$ planes. During the second ECAP pass, however, strain was accommodated primarily by dislocation-glide processes. The specific slip system was strongly dependent on the processing route, i.e., route A, B, or C. Alternating twin bands containing prism **a** and **c** + **a** dislo-

Table 1
Schmid factors for various slip mechanisms following different processing routes ([10$\bar{1}$4] is chosen as the normal direction on Z plane after the first pass of ECA pressing)

		a slip on basal plane	a slip on prismatic plane	a+c slip on pyrimidal plane
Route C	Matrix	0.11	0.06	0.48
	Twinned region	0.21	0.25	0.21
Route B	Matrix	0.22	0.41	0.21
	Twinned region	0.21	0.39	0.21
Route A	Matrix	0.07	0.08	0.39
	Twinned region	0.43	0.23	0.22

cations characterized deformation via route C, but basal **a** slip with deformation micro-twins comprised the mechanism via route A. However, prism **a** slip was the main deformation mechanism in every twin band in route B. These results suggest that the texture formed during the first pass and the resolved shear stress for each slip system determine the deformation mechanism during the second ECAP pass and thus must be carefully considered in understanding microstructure development during equal-channel angular pressing.

Acknowledgements

The authors gratefully acknowledge the support of the Air Force Officice of Scientific Research and its Asian Office of Aerospace Research and Development (Drs K.C. Goretta and C.S. Hartley, program managers).

References

[1] Berbon PB, Furukawa M, Horita Z, Nemoto M, Tsenev NK, Valiev RZ, Langdon TG. Mater. Sci. Forum 1996;217:1013.
[2] Valiev RZ, Salimonenko DA, Tsenev NK, Berbon PB, Langdon TG. Scripta mater. 1997;37:1945.
[3] Shin DH, Kim WJ, Choo WY. Scripta mater. 1999;41:259.
[4] Shin DH, Kim BC, Kim YS, Park KT. Acta mater. 2000;48:3245.
[5] Iwahashi Y, Furukawa M, Horita Z, Nemoto M, Langdon TG. Metall Mater Trans 1998;A29:2245.
[6] Valiev RZ, Alexandrov IV. Nanostruct Mater. 1999;12:35.
[7] Berbon PB, Tsenev NK, Valiev RZ, Furukawa M, Horita Z, Nemoto M, Langdon TG. Metall. Mater. Trans. 1998;29A:2237.
[8] Semiatin SL, Segal VM, Goetz RL, Goforth RE, Hartwig KT. Scpita metall. mater. 1995;33:535.
[9] Nemoto M, Horita Z, Furukawa M, Langdon TG. Metals Mater. 1998;4:1184.
[10] Segal VM. Mater. Sci. Eng. 1995;197:157.
[11] Stolyarov VV, Zhu YT, Lowe TC, Valiev RZ. Mater. Sci. Eng. 2001;A303:82.
[12] Mabuchi M, Ameyama K, Iwasaki H, Higashi K. Acta mater. 1999;47:2047.
[13] Mukai T, Yamanoi M, Watanabe H, Higashi K. Scripta mater. 2001;45:89.
[14] Yamashita A, Horita Z, Langdon TG. Mater. Sci. Eng. 2001;A300:142.
[15] Kim WJ, An CW, Kim YS, Hong SI. Scripta mater. 2002;47:39.
[16] Horita Z, Matsubara K, Makii K, Langdon TG. Scripta mater. 2002;47:255.
[17] Furukawa M, Iwahashi Y, Horita Z, Nemoto M, Langdon TG. Mater. Sci. Eng. 1998;257:328.
[18] Iwahashi Y, Horita Z, Nemoto M, Langdon TG. Acta mater. 1997;45:4733.
[19] Iwahashi Y, Horita Z, Nemoto M, Langdon TG. Acta mater. 1998;46:3317.
[20] Yoo MH. Metall. Trans. 1981;A12:409.
[21] Paton NE, Backofen WA. Metall. Trans. 1970;1:2839.
[22] Akhtar A. Metall. Trans. 1975;A6:1105.
[23] Minonishi Y, Morozumi S, Yoshinaga H. Scripta metall. 1982;16:427.
[24] Numakura H, Koiwa M. Metall. Sci. Technol. 1998;16:4.
[25] Delo DP, Semiatin SL. Metall. Mater. Trans. 1999;30:2473.
[26] Zhu YT, Lowe TC. Mater. Sci. Eng. 2000;A291:46.
[27] Iwahashi Y, Wang J, Horita Z, Nemoto M, Langdon TG. Scripta mater. 1996;35:143.
[28] Semiatin SL, Segal VM, Goforth RE, Frey ND, DeLo DP. Metall. Mater. Trans. 1999;30:1425.
[29] Shin DH, Kim I, Kim J, Park KT. Acta mater. 2001;49:1285.

[30] Kim J, Kim I, Shin DH. Scripta mater. 2001;45:575.
[31] Paton NE, Backofen WA. Trans. Am. Inst. Min. Engrs 1969;245:1369.
[32] Kalidindi SR. J. Mech. Phys. Solids 1988;46:267.
[33] Christian JW, Mahajan S. Prog. Mater. Sci. 1995;39:1.
[34] Semiatin SL, DeLo DP. Mater. Design 2000;21:311.
[35] Pond RC, Bacon DJ, Serra A, Sutton AP. Metall. Trans. 1991;A22:1185.
[36] Shin DH, Kim I, Kim J, Zhu YT. Mater. Sci. Eng. 2002;A334:239.
[37] Madhava NM, Worthington PJ, Armstrong RW. Phil. Mag. 1972;25:519.
[38] Armstrong RW, Worthington PJ. In: Rhode RW, Butcher BM, Holland JR, Karnes CH, editors. Metallurgical effects at high strain rates. New York: Plenum Publ. Corp.; 1974. p. 40-1.
[39] Meyers MA, Voehringer O, Chen KY. In: Ankem S, Pande CS, editors. Advances in twinning. Pennsylvania: Publication of TMS; 1999. p. 4-3.

Chapter 3: Effects of temperature and initial microstructure on the equal channel angular pressing of Ti-6Al-4V alloy

PERGAMON

Scripta Materialia 48 (2003) 197–202

Scripta MATERIALIA

www.actamat-journals.com

Effects of temperature and initial microstructure on the equal channel angular pressing of Ti–6Al–4V alloy

Y.G. Ko [a], W.S. Jung [b], D.H. Shin [b], C.S. Lee [a,*]

[a] *Department of Materials Science and Engineering, Center for Advanced Aerospace Materials, Pohang University of Science and Technology, Pohang 790-784, South Korea*

[b] *Department of Metallurgy and Materials Science, Hanyang University, Ansan, Kyunggi-Do, 425-791, South Korea*

Received 10 June 2002; received in revised form 29 July 2002

Abstract

Equal channel angular pressing of Ti–6Al–4V alloy was successfully carried out isothermally above 600 °C. The equiaxed microstructure presented more uniform material flow than the Widmanstätten microstructure, which was discussed in relation to flow softening behavior of the two microstructures.
© 2002 Acta Materialia Inc. Published by Elsevier Science Ltd. All rights reserved.

Keywords: Equal channel angular pressing; Ti–6Al–4V alloy; Microstructure; Flow softening

1. Introduction

The equal channel angular (ECA) pressing technique, one of severe plastic deformation processes, is generating great interest now-a-days due to its commercial potential for producing bulk ultra fine-grained (UFG) materials, which may exhibit enhanced strength and superplastic properties [1]. Compared to other conventional forming methods such as rolling, extrusion, and drawing, the ECA pressing technique has two distinct advantages. The first is that it imposes much higher plastic strain during single pressing, and the second is that it produces UFG materials without reducing the available dimensions for working parts. In this regard, active research efforts have been made recently, and successful applications have been reported for various materials such as Al [2], Fe [3,4], and Ti [5].

However, earlier research concentrated on single-phase materials that exhibit higher ductility. Considering the industrial importance of two-phase materials, it is essential to establish optimum processing conditions of such difficult-to-fabricate materials. Recently, DeLo and Semiatin [6] investigated hot working of Ti–6Al–4V alloy via ECA pressing under non-isothermal conditions, but found significant amounts of surface segments in both equiaxed and Widmanstätten microstructures after deforming the preheated (exceeding 900 °C) billets.

In this study, we investigated the optimum pressing temperatures under isothermal conditions. It was also pertinent to study the effect of initial microstructure on the formability of

* Corresponding author. Tel.: +82-54-279-2141; fax: +82-54-279-2399.

E-mail address: cslee@postech.ac.kr (C.S. Lee).

1359-6462/03/$ - see front matter © 2002 Acta Materialia Inc. Published by Elsevier Science Ltd. All rights reserved.
PII: S1359-6462(02)00356-1

Ti–6Al–4V alloy. Finally, the microstructural evolution process was investigated by using transmission electron microscopy to verify the grain refinement of ECA pressed Ti–6Al–4V alloy.

2. Experimental procedures

The material used in this study was Ti–6Al–4V alloy with a chemical composition of 6.03Al, 3.83V, 0.2Fe, 0.19O, 0.01C, 0.007N in weight percent and balance titanium. The as-received bimodal microstructure was heat treated at 950 °C for 2 h and furnace cooled, resulting in an equiaxed microstructure with an average α grain size of 11 μm. Widmanstätten microstructure was obtained, when the as-received alloy was heat treated at 1050 °C for 1 h and furnace cooled, representing an average colony size of 300 μm and a lamellar spacing of 4.0 μm.

Rod type specimens (9.5 mm in diameter and 80 mm in height) were machined for ECA pressing. To determine the optimum pressing temperature, ECA pressing was carried out isothermally at 500, 600, and 700 °C, respectively, for the Widmanstätten microstructure. The present die was designed to yield an effective strain of ~1 [4,7]. To reduce the friction between the die and the specimen during ECA pressing, graphite powders were used as a lubricant. And the specimens were rotated 180° around their longitudinal axis between ECA pressings [4]. Hot compression tests were also carried out using a Gleeble 3800 machine at 600 °C to compare the deformation characteristics of equiaxed and Widmanstätten microstructures. Rod type specimens (10 mm in diameter and 12 mm in height) were compressed at a strain rate of 0.3/s until the height decreased up to 50%. Deformed specimens were sectioned along the compression (or pressing) axis, and the microstructures were analyzed by optical microscopy and transmission electron microscopy.

3. Results and discussion

3.1. Effect of isothermal pressing temperature

Fig. 1 shows the macroscopic sections of Widmanstätten microstructures, which experienced a single ECA pressing pass under isothermal conditions at three different temperatures. At a low temperature of 500 °C, deformation was severely localized with pronounced shear bands and shear fractures (Fig. 1a), while deformation at high temperatures of 600 and 700 °C produced relatively uniform deformation throughout the specimens (Fig. 1b and c). There was no significant difference in the macroscopic feature between specimens pressed at 600 and 700 °C. This temperature of 600 °C for the uniform flow obtained in this study is quite low compared to those of earlier works [6]. These works reported that flow localization and fracture occur even at 900–985 °C. They performed ECA pressing under non-isothermal conditions, i.e., pressing the high temperature billets into a low temperature die (300 °C), which induced heat transfer from the specimen to

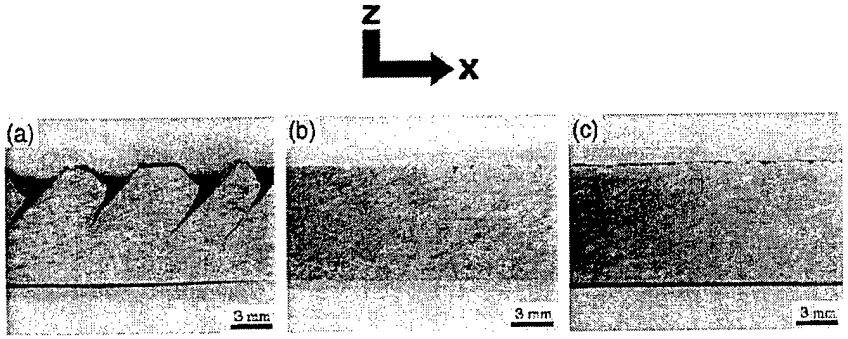

Fig. 1. Macrographs of Widmanstätten microstructure after a single ECA pressing at isothermal temperatures of (a) 500 °C, (b) 600 °C, and (c) 700 °C, respectively. The arrow indicates pressing direction.

the die during ECA pressing. Consequently, the temperature of specimen surfaces dropped significantly, resulting in the formation of segments at the specimen surface. In contrast, our study performed under isothermal conditions did not show any noticeable segments at the surface even at much lower temperatures (600–700 °C) compared to those under non-isothermal conditions. However, increasing the die temperature to 600 °C is not desirable in practical situation, since it can reduce die life significantly. Therefore, the roles of other processing variables (such as strain or strain rate) or microstructural factors (such as initial microstructures) on ECA pressing temperature have to be investigated.

3.2. Effect of initial microstructure

To understand the role of initial microstructure on ECA pressing of Ti–6Al–4V alloy, the equiaxed and Widmanstätten microstructures were pressed isothermally at 600 °C. Fig. 2 shows microstructures and surface quality of two microstructures after a single pressing at 600 °C. Fig. 2a and b show two microstructures elongated along the shear direction and making an angle of 25–30° to the pressing direction. However, initial morphology was not significantly changed, revealing relatively uniform deformation in both microstructures. Comparing the surface quality of two bars, the equiaxed microstructure represented a smoother

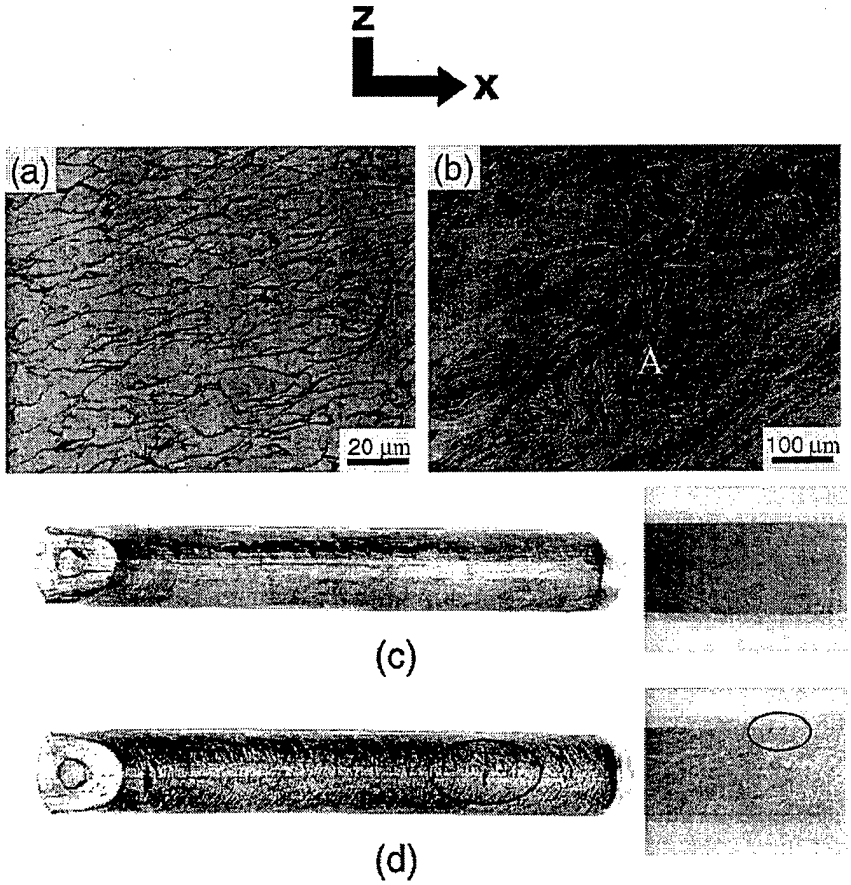

Fig. 2. Microstructures and surfaces after a single ECA pressing: (a,c) equiaxed and (b,d) Widmanstätten microstructure. The pressing direction is from left to right. Mark 'A' shows lamellae kinking and bending in the Widmanstätten microstructure.

surface than the Widmanstätten microstructure, which was in line with the observations of DeLo and Semiatin [6].

Widmanstätten microstructure represented poorer surface quality than the equiaxed microstructure. Because the colony size of Widmanstätten microstructure is much larger than the grain size of the equiaxed microstructure, planar slip deformation will occur easily in the Widmanstätten microstructure, inducing severe flow localization at colony boundaries and/or prior β boundaries. Consequently, the tendency for the formation of segments on the surfaces is expedited in the Widmanstätten microstructure. In earlier work on non-uniform flow, Segal [8] explained that unsteady flow might result from material softening and geometrical instability of the shear plane. However, his results could not provide sufficient explanation for flow localization phenomena in relation to microstructural factors. In this study, it was found that flow softening was closely associated with the microstructural change (for example, curling or bending of lamellae in the Widmanstätten microstructure) during the deformation. Recently, DeLo and Semiatin [6] investigated strain non-uniformity during ECA pressing of Ti–6Al–4V alloy, and reported that flow localization might be closely related to flow softening, i.e., the decrease of flow stress with an increase in strain. They used a flow-localization parameter, α_S suggested by Semiatin and Jonas [9], to quantify the degree of flow softening behavior. The brief description of α_S is given in Eq. (1).

$$\alpha_S \equiv \left(\frac{1}{\varepsilon}\right)\left(\frac{d\varepsilon}{d\varepsilon}\right) - -\left\{\left(\frac{\partial \ln\sigma}{\partial\varepsilon}\right)\Big|_{\varepsilon,T} + \left(\frac{\partial\sigma}{\partial T}\right)\Big|_{\varepsilon,\varepsilon}\left(\frac{1}{\sigma}\frac{dT}{d\varepsilon}\right)\right\}\Big/ m, \quad (1)$$

where m is the strain rate sensitivity. The value of α_S must always be positive for flow localization to occur. The first term on the right-hand side in Eq. (1) relates to microstructure, and the second term is associated with the amount of heat transfer by temperature change during deformation. The estimation on α_S can be simplified if the second term (indicating heat generation during the deformation) is negligible. In this study, the second term was neglected for the following two reasons. Present study on ECA pressing was carried out isothermally so that the specimen always kept its targeted temperature. Furthermore, according to the heat generation experiment using pure Al, temperature increase corresponded to about 40 °C with a pressing speed of 18 mm/s, and 0.3 °C with 0.18 mm/s [10] which did not affect deformation behavior. The pressing speed used in this study was 2 mm/s, which would generate only several degrees of temperature, if any. From the aforementioned points, the α_S can be simplified as in Eq. (2).

$$\alpha_S - -\left\{\left(\frac{d\ln\sigma}{d\varepsilon}\right)\Big|_{\dot{\varepsilon}}\right\}\Big/ m. \quad (2)$$

In order to obtain a meaningful α_S value, it is important to carry out ECA pressing under isothermal condition. However, earlier work [6] estimated the α_S based on experimental data carried out under a non-isothermal condition that led to heat transfer between the workpiece and the die, resulting in a significant drop of workpiece temperatures during ECA pressing. Table 1 lists flow-localization parameter (α_S) values obtained by hot compression tests. Both equiaxed and Widmanstätten microstructures represented positive α_S values, indicating that flow softening (and consequent flow localization) would occur in both microstructures. However, it is important to notice that α_S of the Widmanstätten microstructure is approximately twice as large as that of the equi-

Table 1
ECA pressing condition (600 °C, 0.3 s^{-1}) and deformation characteristics of equiaxed and Widmanstätten microstructures in relation to the flow-localization parameter (α_S)

	Equiaxed	Widmanstätten
$\frac{d\ln\bar{\sigma}}{d\bar{\varepsilon}}$	−0.091[a]	−0.152[a]
m	0.059	0.039
α_S	1.54	3.90
Microstructure after a single pass of ECA pressing	Uniform flow	Segments

[a] $\frac{d\ln\bar{\sigma}}{d\bar{\varepsilon}}$ was determined at $\bar{\varepsilon} \approx 0.3$.

axed microstructure, which agrees well with the experimental results shown in Fig. 2c and d.

3.3. Microstructural evolution

In order to ascertain how microstructures change during ECA pressing of Ti–6Al–4V alloy, equiaxed microstructures with superior surface quality were pressed isothermally with 4 ECA pressings at 600 °C. Fig. 3 shows bright field (BF) images of α phase by increasing the number of pressing operations. Fig. 3a shows the initial microstructure with a low dislocation density. After a single ECA pressing, long parallel shear bands (0.2–0.3 μm in width) were observed in the microstructure (Fig. 3b). These boundaries were thought to be low-angle boundaries because the corresponding selected area diffraction (SAD) pattern comprised relatively regular spots. The microstructure after two ECA pressings consisted of equiaxed α grains with an average diameter of 0.4 μm, while most of the parallel bands disappeared (Fig. 3c). The corresponding SAD pattern started to form a ring pattern with diffused spots. The spreading of the diffraction spots indicates that the misorientation of boundaries is fairly large. After 4 ECA pressings, more refined equiaxed α grains (0.2–0.3 μm in diameter) were observed (Fig. 3d). From the ring pattern of the diffraction spots, it was inferred that most refined grains consisted of high angle grain boundaries. However, many boundaries were not clearly defined and showed some extinction contours inside the grains (Fig. 3d), implying that microstructure is not stabilized. In contrast, β phase grains easily fragmented with an increase in ECA pressings (Fig. 4a and b). This phenomenon is attributed to the following: (a) low volume fraction of β phase (10%), (b) thin strip morphology of β phase, and (c) less capability of β phase to accommodate severe plastic strains than α phase at 600 °C [11]. Detailed investigations on deformation characteristics, grain refinement mechanisms and refined grain stability are in progress.

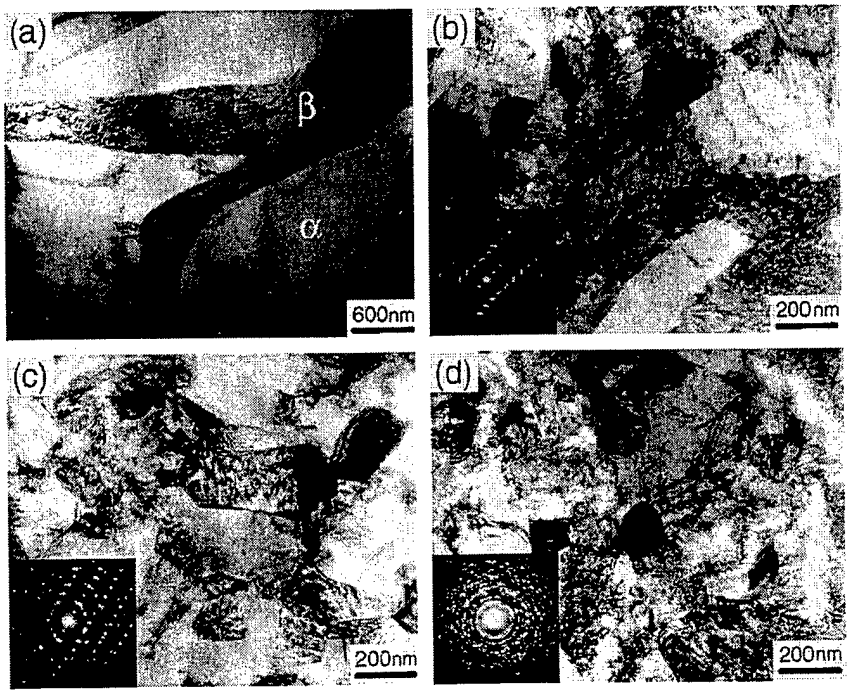

Fig. 3. TEM micrographs and SAD patterns of α phase in equiaxed microstructure showing microstructural evolution: (a) as-received, (b) 1 pass, (c) 2 passes, and (d) 4 passes of ECA pressing.

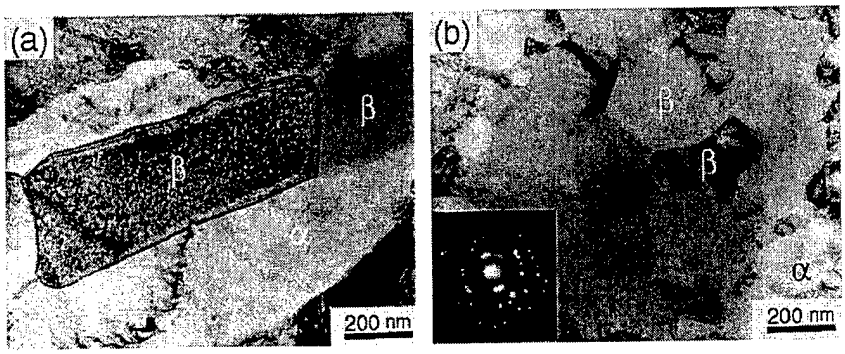

Fig. 4. TEM micrographs of β phase in an equiaxed microstructure showing microstructural evolution after: (a) 1 pass and (b) 4 passes of ECA pressing.

4. Summary

1. ECA pressing was successfully carried out isothermally at 600 and 700 °C for both the equiaxed and Widmanstätten microstructures of Ti–6Al–4V alloy.
2. After a single ECA pressing at 600 °C, the equiaxed microstructure showed smoother surfaces and more uniform material flow than the Widmanstätten microstructure.
3. A flow-localization parameter (α_S) was used to quantify flow softening amount for equiaxed and Widmanstätten microstructures. The α_S of the Widmanstätten microstructure was approximately twice as large as that of the equiaxed microstructure, which agrees well with the experimental results.
4. By increasing the number of ECA pressings, most α and β grains were significantly refined, revealing grains 0.2–0.3 μm in diameter consisting of high angle grain boundaries.

Acknowledgements

This work was supported by a grant from the Korea Science and Engineering Foundation and the Center for Advanced Aerospace Materials, POSTECH. One of the authors (DHS) is also grateful for support from the Air Force Office of Scientific Research/Asian Office of Aerospace Research and Development.

References

[1] Valiev RZ, Islamgaliev RK, Alexandrov IV. Prog Mater Sci 2000;45:103.
[2] Iwahashi Y, Horita Z, Nemoto M, Langdon TG. Acta Mater 1998;46:3317.
[3] Valiev RZ, Ivanisenko YV, Rauch EF, Baudelet B. Acta Mater 1996;44:4705.
[4] Shin DH, Kim BC, Kim YS, Park KT. Acta Mater 2000;48:2247.
[5] Stolyarov VV, Zhu YT, Alexandrov IV, Lowe TC, Valiev RZ. Mater Sci Eng A 2001;299:59.
[6] DeLo DP, Semiatin SL. Metall Trans A 1999;30:2473.
[7] Iwahashi Y, Wang J, Horita Z, Nemoto M, Langdon TG. Scripta Mater 1996;35:143.
[8] Segal VM. Mater Sci Eng A 1999;271:322.
[9] Semiatin SL, Jonas JJ. Formability and workability of metals. Metals Park, OH: ASM; 1984.
[10] Yamaguchi D, Horita Z, Nemoto M, Langdon TG. Scripta Mater 1999;41:791.
[11] Partridge PG. The crystallography and deformation mode of HCP metals. in Met Rev 1968;118:169.

Chapter 4: Future work

We believe that the aforementioned results achieved with the grant from the AOARD constitute a significant contribution to a fundamental understanding on the processing science necessary to produce ultra-fine grained (UFG) Ti and Ti-6Al-4V alloy using ECAE process. For application of the knowledge accumulated through the research to an actual processing of the alloys, however, a further study is needed in several areas.

First, the texture formed during the first pass of ECAE of CP Ti must be investigated in order to control the grain refining route. The texture was observed to be associated mainly with the deformation twins. ECAE of the Ti at various temperatures, however, revealed that twinning is the predominant deformation mechanism only when the processing temperature is around 400°C. ECAE at temperatures higher or lower than 400°C resulted in plastic deformation via dislocation gliding. Currently, the change in deformation mechanism, and its influences on grain refinement and mechanical properties of pure titanium have not been understood clearly so far. This should provide some guidance for enhanced improvements in mechanical properties of commercially pure titanium.

Secondly, the effect of microstructure of Ti-6Al-4V alloy on the localized shear deformation must be investigated further. A severe localized deformation in the ECAEed alloy was observed in the alloy with Widmanstätten microstructure. The sample with equiaxed microstructure, on the other hand, was deformed uniformly through the processing. The mechanism of localized shear bands formation during the ECAE must be controlled in order to obtain uniform deformation of the alloy.

Finally, the superplasticity of Ti-6Al-4V alloy with submicron grains at higher strain rate would be a worthwhile pursuit. The results in the previous year revealed that the temperature of superplasticity could be decreased by more than 250°C with the sample processed by ECAE route. For practical application of the sample, however, it is necessary to obtain the superplasticity at higher strain rates.